Metastatic Renal Clear Cell Carcinoma First Presenting As a Head-and-Neck Mass: two case reports

Authors

Xinyao Han, Hui Huangfu

Correspondence

13934518228@163.com (H. Huangfu)

Graphical Abstract

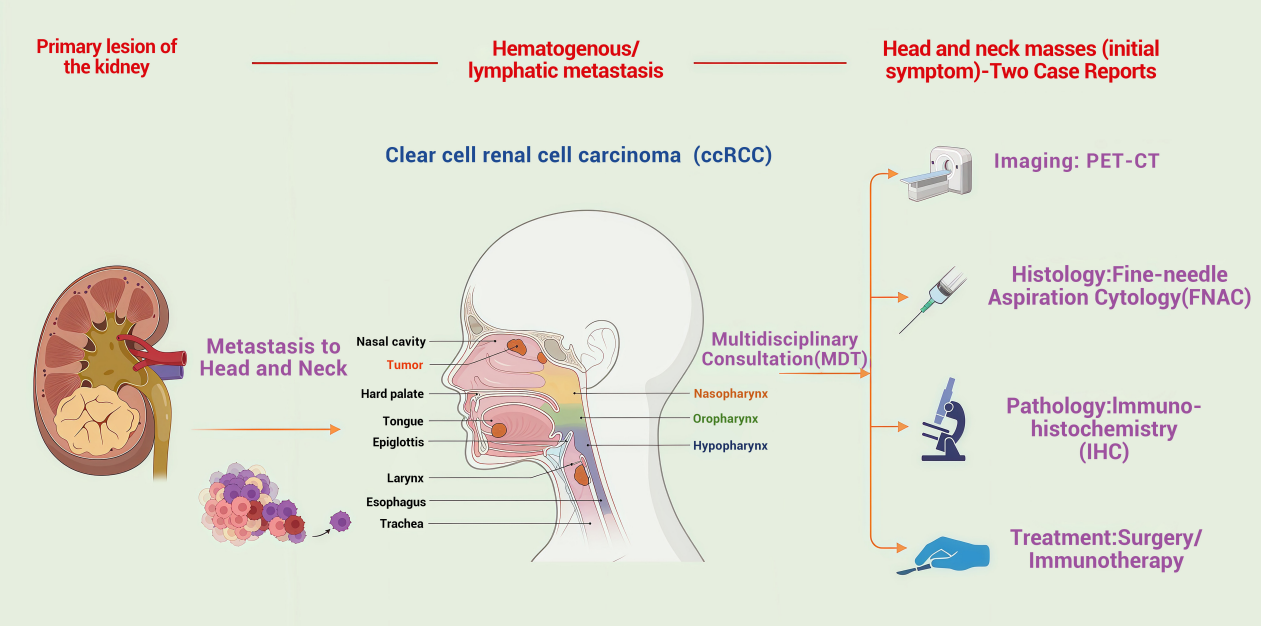

https://doi.org/10.71321/1ckasv14

Metastatic Renal Clear Cell Carcinoma First Presenting As a Head-and-Neck Mass: two case reports

Xinyao Han[1] , Hui Huangfu[2*]

Received: 2026-01-15 | Accepted: 2026-03-09 | Published online: 2026-03-22

Abstract

Background: Clear cell renal cell carcinoma (ccRCC) is a prevalent malignant tumor within the urinary system, characterized by a high metastatic potential. However, instances of ccRCC metastasizing to the head and neck are exceedingly rare.

Case presentation: This article presents two patients who were admitted to the Department of Otorhinolaryngology Head and Neck Surgery. Case 1: A 61-year-old East Asian male patient presented with a painless, progressive enlargement of the left neck. Imaging revealed a 3.6 × 2.3 cm enhancing solid lesion with cystic components in the deep lobe. After surgical resection, histopathology with immunohistochemistry ($CD10^{+}$, $vimentin^{+}$) suggested metastatic clear cell carcinoma of renal origin. Subsequent Positron Emission Tomography-Computed Tomography (PET CT) confirmed a left renal mass (11.4 × 10.1 cm, SUVmax 5.86) with ipsilateral lung nodules, establishing the diagnosis of ccRCC with parotid and pulmonary metastases. Case 2: Another 69-year-old East Asian male patient presented to the hospital with a complaint of foreign body sensation in the pharynx. This individual had previously undergone laparoscopic left nephrectomy for left renal cell carcinoma 14 years prior. Subsequent electronic laryngoscopy identified a new growth on the right side of the pharyngeal wall, leading to laryngoscopic resection of the lesion. Postoperative pathology indicated metastatic clear cell carcinoma originating from the renal site.

Conclusion: Both cases involved metastatic lesions of ccRCC in the head and neck region, underscoring the critical importance of promptly conducting PET-CT scans and relevant pathological assessments when encountering head and neck masses with unidentified primary origins to ascertain whether they represent metastatic clear cell renal cell carcinoma(mCCRCC). The vague initial clinical manifestations of mCCRCC pose significant obstacles to its early clinical detection, necessitating multidisciplinary consultations, prolonged patient monitoring, and the administration of postoperative radiotherapy, chemotherapy, immunotherapy, and other interventions to enhance patient survival rates.

Keywords: clear cell renal cell carcinoma; head and neck metastasis; parotid; oropharyngeal mass

Introduction

Renal cell carcinoma (RCC) is one of the most lethal malignancies in the urinary system and exhibiting a propensity for head and neck metastasis following breast and lung cancers [1]. Clear cell renal cell carcinoma (ccRCC), chromophobe renal cell carcinoma (chRCC), and papillary renal cell carcinoma (pRCC) are distinct subtypes of RCC. Among these subtypes, ccRCC is the predominant histological subtype, accounting for approximately 75% of all RCC diagnoses, known for its aggressive nature, high metastatic potential, and elevated recurrence rates [2]. Studies indicate that 30% of patients have metastases at diagnosis [3], and another 25–40% will develop metachronous metastases after nephrectomy [4].The most frequent sites of metastasis in RCC include the lungs (76%), bones (42%), and liver (41%). In contrast, metastasis to the head and neck is exceedingly rare, affecting regions such as cervical lymph nodes (48%), paranasal sinuses (34%), thyroid (14%), skull (10%), parotid glands (5%), tongue (5%), and facial skin (5%) [5]. In a large series of 671 RCC patients, only one case of parotid metastasis was documented [6]. This article presents two cases of ccRCC metastasizing to the head and neck, while also examining their clinical features and treatment strategies. Herein we describe two unusual presentations of ccRCC initially manifesting as head and neck masses: one in the deep lobe of the parotid gland and one in the lateral oropharyngeal wall 14 years after nephrectomy. These cases highlight the diagnostic challenges and underscore the importance of a thorough metastatic work up and long term surveillance.

1 First Clinical Medical College, Shanxi Medical University, Taiyuan, Shanxi ,China

2 Department of Otorhinolaryngology-Head and Neck Surgery, First Hospital of Shanxi Medical University, Taiyuan, Shanxi, China

* Corresponding Author.

Case presentation

Case 1: A 61-year-old East Asian male patient was admitted to the hospital following the discovery of a painless mass in the left parotid gland three weeks prior. He reported no discomfort, including pain, fever, weight loss, or facial paralysis. The patient has a 20-year history of hypertension, which is well-managed with regular treatment and effective blood pressure control. There is no family history of hereditary diseases. A specialized examination revealed a hard, painless mass approximately 4 cm in diameter in the left parotid gland region, characterized by well-defined boundaries and normal mobility. The bilateral neck appeared asymmetrical, with no palpable enlarged lymph nodes. There were no signs of inflammation or local infection on the skin, facial nerve function was intact, and the examination of the remaining cranial nerves showed no significant abnormalities.

To clarify the diagnosis, comprehensive laboratory and imaging examinations were conducted. Initial laboratory tests showed no significant abnormalities, including complete blood count, renal function tests, liver function tests, electrolyte levels, coagulation, and infectious disease screening. Ultrasound of the salivary glands and cervical lymph nodes detected a cystic and solid mass in the upper region of the left parotid gland measuring 3.2 × 2.8cm, with a clear boundary and regular shape. The solid component exhibited rich vascular distribution, indicating a potential mixed tumor (Figure 1). Plain scan and enhanced computed tomography (CT) of the soft tissue in the neck revealed a clearly demarcated lesion in the left parotid gland region, measuring approximately 3.6 × 2.3 cm, exhibiting significantly uneven enhancement. Within this lesion, multiple non-enhanced cystic cavities were identified, and a "marginal vascular sign" was noted surrounding the lesion. The enhancement degree diminished during the venous phase, demonstrating a "fast-in and fast-out" enhancement pattern. The soft tissue structures of both sides of the neck appeared symmetrical, with no evident abnormalities in size, shape, or density. Additionally, no conspicuous enlarged lymph node shadows were detected in either side of the neck, raising the possibility of adenolymphoma (Figure 2). Fine needle aspiration cytology (FNAC) was considered but not performed because the lesion was deeply situated and highly vascular (Grade 3 flow), raising concerns for both hemorrhage risk and sampling inadequacy. Furthermore, while the encapsulated appearance reduced the likelihood of tumor seeding, the potential for dissemination if malignant could not be completely ruled out. Therefore, after discussion with the patient who preferred definitive surgical management, direct excision with intraoperative frozen section was undertaken.

Differential diagnosis before surgery: Warthin tumour, pleomorphic adenoma, salivary duct carcinoma, and metastasis (especially in view of the hypervascular features). Because of the absence of known primary cancer, metastatic disease was considered less likely but not excluded. The patient underwent the necessary preoperative examinations and subsequently had surgery under general intravenous combined anesthesia on December 18, 2024. During the procedure, the tumor was identified in the deep lobe of the left parotid gland. It was solid, encapsulated, and measured approximately 4.0 × 4.0 × 3.0cm, with indistinct margins from the surrounding tissues, a brittle texture, and a tendency to bleed. The left common trunk of the facial nerve was dissected under facial nerve monitoring. After ensuring the protection of each branch of the facial nerve, the deep lobe mass of the parotid gland was excised. Intraoperative frozen section analysis suggested a low-grade malignant salivary gland tumor, prompting the resection of the surrounding glandular tissue.

Figure 1. Ultrasound: Left parotid 3.2×2.8 cm cystic-solid mass with thick walls, internal septations, and rich vascularity (Color Doppler Grade 3). Scale bar = 1 cm. Arrow indicates mass.

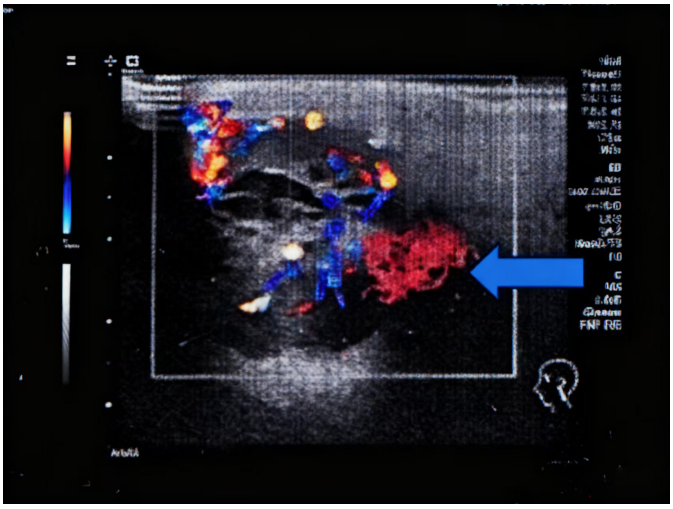

Figure 2. CT neck with contrast: Axial arterial phase showing 3.6×2.3 cm heterogeneously enhancing left deep parotid mass with "fast-in fast-out" pattern and peripheral vascular rim (arrow).

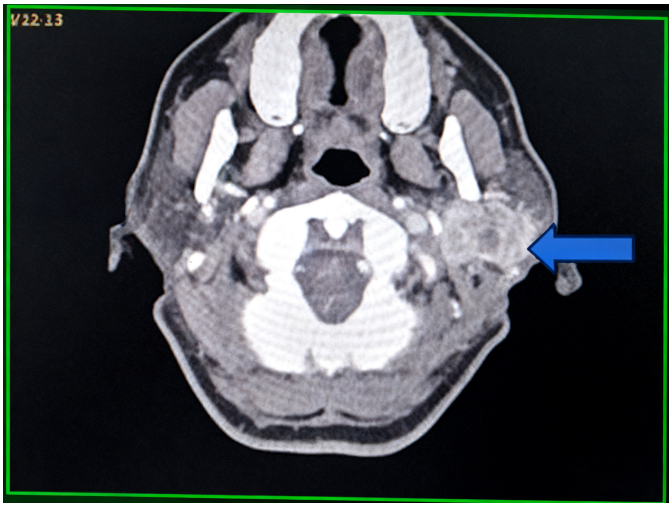

Postoperative histopathological examination, complemented by immunohistochemical (IHC) phenotyping, revealed tumor cells organized into nest-like clusters characterized by moderate cell size, clear cytoplasm, and marked hemorrhage. IHC analysis demonstrated strong positivity for PAX8, CD10, vimentin, and carbonic anhydrase IX (CAIX), while the tumor cells were negative for CK7, p63, p40, S100, SOX10, and GATA. The Ki-67 proliferation index was 10% (Figure 3 and Figure 4). A consultation with the urology department recommended a comprehensive PET-CT examination. Postoperative PET-CT revealed a left renal mass measuring 11.4 × 10.1 cm with

heterogeneous enhancement and increased FDG uptake (SUVmax 5.86), demonstrating perinephric fat invasion consistent with T3a disease. Metastatic involvement was identified in the left parotid surgical bed (SUVmax 7.39) and bilaterally in the lungs, with the largest nodule located in the posterior basal segment of the left lower lobe measuring approximately 1.2 cm (SUVmax 2.18). No bone metastases were detected, and brain imaging was not performed as the patient remained asymptomatic. Integrating the imaging findings, histopathological analysis, and the patient's medical history, a differential diagnosis was made for various benign and malignant parotid gland masses. Ultimately, the patient was diagnosed with mCCRCC to the parotid gland. Following the diagnosis, the patient was referred to urology and medical oncology for multidisciplinary management. After multidisciplinary team (MDT) discussion, a decision was made to initiate first-line systemic therapy with pembrolizumab plus axitinib, with consideration of cytoreductive nephrectomy after three cycles if a favorable response was achieved. Systemic therapy commenced with pembrolizumab 200 mg intravenously every three weeks and axitinib 5 mg orally twice daily; the axitinib dose was subsequently reduced to 3 mg twice daily after two weeks due to the development of grade 2 hypertension. The first restaging CT scan, performed approximately 8 weeks after treatment initiation and evaluated per RECIST 1.1 criteria, demonstrated a partial response (PR) in the primary renal mass, which measured 8.3 × 7.4 cm, representing a 27% reduction from baseline. The bilateral pulmonary nodules remained stable as non-target lesions, and the parotid surgical bed showed no evidence of local recurrence. The patient's renal function remained stable, with an eGFR of 45 mL/min/1.73 m². The patient is currently alive with disease 10 months after initial presentation, experiencing continuous symptomatic relief, and remains on ongoing systemic therapy with regular imaging surveillance. TNM staging (AJCC 8th edition): cT3aN0M1 (lung, parotid).

Case 2: A 69-year-old East Asian man was hospitalized for a one-week history of a foreign body sensation in the throat. He denied experiencing dry, itchy, or sore throat, or shortness of breath. An electronic laryngoscopy examination identified a new organism on the right pharyngeal lateral wall, measuring approximately 1.0 × 1.0 × 1.0cm, displaying a smooth surface with a small amount of attached pseudomembrane (Figure 5). Palpation during a specialized physical examination did not detect any lymph nodes in the neck. Initial laboratory tests revealed a significant decrease in glomerular filtration rate (47.9 ml/min/1.73 m²) with no other notable abnormalities. The patient has a history of poorly controlled hypertension spanning over two decades. Fourteen years ago, he underwent laparoscopic left nephrectomy due to ccRCC with hemorrhagic cystic changes in the left kidney (pathology: pT1b, Fuhrman grade 2, margins negative). Subsequent annual physical examinations showed no abnormalities in urine routine or renal function.

Following the completion of the necessary preoperative examinations, the patient underwent resection of a pharyngeal lesion with the assistance of a laryngoscope on May 8, 2025. During the procedure, a red solid neoplasm located on the surface of the right pharyngeal palatine arch was excised. Intraoperative cryotherapy indicated that the morphology of this mass was consistent with metastatic clear cell carcinoma of renal origin (Figure 6). The surrounding adherent tissue was also excised to ensure complete resection. Postoperative pathology confirmed the diagnosis of mCCRCC. The patient had a pathologically confirmed history of left ccRCC treated with nephrectomy 14 years earlier, and intraoperative frozen

Figure 3. H&E stain, low power (×40): Nested architecture of clear cells with delicate vascular network and focal hemorrhage. Scale bar = 500 μm.

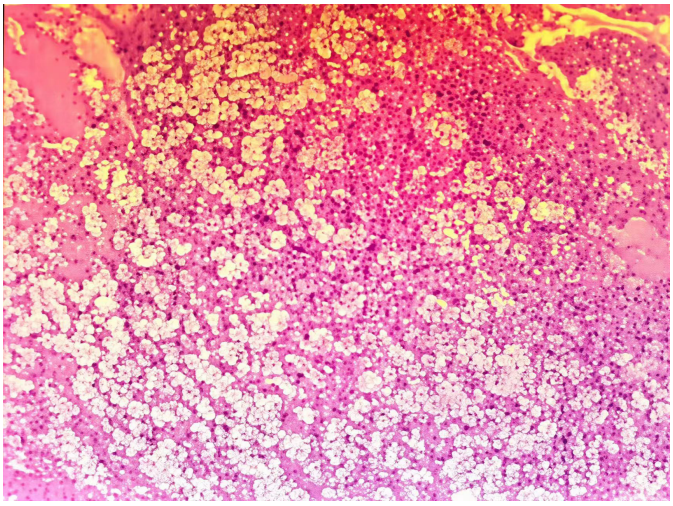

Figure 4. H&E stain, high power (×400): Clear cytoplasm with distinct cell borders, round nuclei, prominent nucleoli. Red blood cells in interstitium. Scale bar = 50 μm.

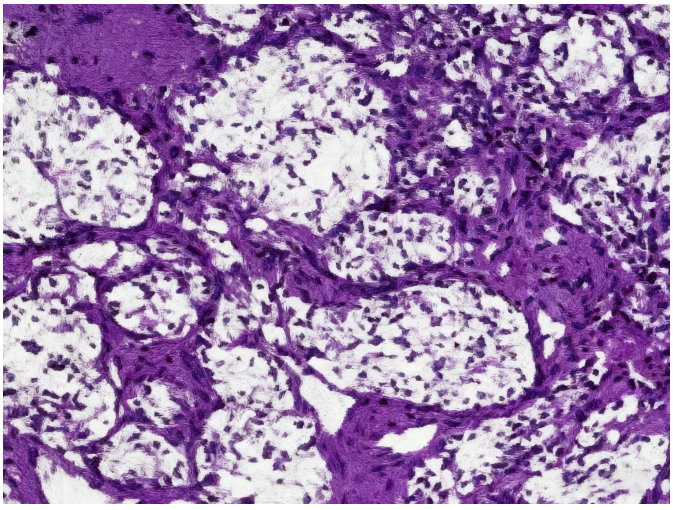

Figure 5. Laryngoscopic view: Smooth, reddish, submucosal mass on right lateral oropharyngeal wall, measuring 1.0×1.0 cm, with small pseudomembrane.

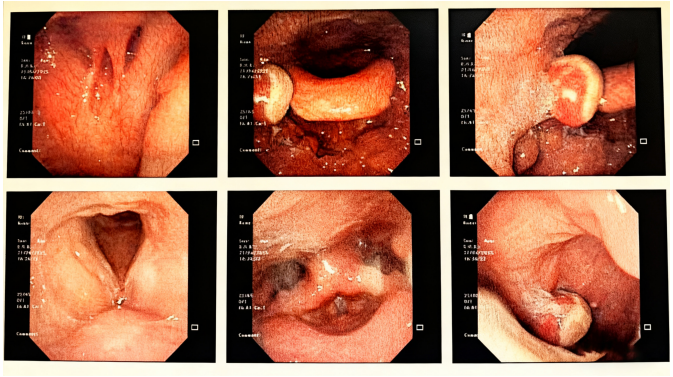

section of the oropharyngeal lesion revealed classic clear cell morphology, which was subsequently confirmed on routine histopathology. Given the definitive history of ccRCC and the characteristic pathological features, the diagnosis was considered sufficiently established at that time. Furthermore, due to the patient's advanced age (69 years) and pre-existing chronic kidney disease stage 3 (eGFR 47.9 mL/min/1.73 m²), the clinical team had concerns about the potential nephrotoxicity of iodinated contrast agents required for PET-CT or contrast-enhanced CT. After thorough discussion with the patient and his family, a decision was made to proceed with close surveillance following complete local excision rather than immediate extensive staging investigations. Additional immunohistochemical markers—such as PAX8, CK7, p63, p40, S100, and SOX10—were not pursued at that time due to resource considerations and the perceived diagnostic certainty based on the strong clinical and pathological correlation.

Following MDT consultation, the patient was staged as pTxN0M1 (solitary oropharyngeal metastasis) according to the AJCC 8th edition, with the current recurrence classified as distant metastasis (M1) given the 14-year interval since the original nephrectomy. After discussion at a MDT board, the medical oncology team recommended adjuvant systemic therapy with nivolumab plus cabozantinib as the preferred option for intermediate-risk recurrence, versus observation, acknowledging that the prolonged latency might suggest an aggressive clone with high metastatic potential. The patient elected active treatment and initiated therapy with nivolumab 240 mg intravenously every two weeks plus cabozantinib 40 mg orally daily; the cabozantinib dose was reduced to 20 mg daily due to baseline chronic kidney disease. The first restaging evaluation, performed approximately 8 weeks after treatment initiation and assessed per RECIST 1.1 criteria, demonstrated no measurable disease (status post-surgical resection) and no new lesions. Treatment was continued as an adjuvant approach. As of the most recent follow-up, the patient remains stable with no evidence of disease progression and continues on regular imaging surveillance. Additionally, we have created detailed clinical timelines for both cases (Table 1 and Table 2), which include all key events from initial presentation through diagnosis, treatment, and follow-up. The timelines are presented in a clear chronological format with approximate dates and corresponding clinical events.

Discussion

We report two exceptional cases of ccRCC presenting initially as head and neck masses: one in the parotid deep lobe and one isolated oropharyngeal metastasis 14 years after nephrectomy. Both presentations are extraordinarily rare; only a handful of similar cases have been reported. A summary of the most relevant published cases is presented in Table 3.

mCCRCC presenting with head and neck space-occupying lesions as the initial manifestation is exceptionally uncommon in clinical practice, representing only 13% of distant metastasies of RCC [6]. Most head and neck metastatic tumors stem from primary lesions in the upper digestive or respiratory tracts, with metastases from distant primary sites, such as renal tumors, being infrequent. Due to the kidney receives 25% of the circulating blood volume, RCC, a hypervascular tumor

Figure 6. H&E stain (×200): mCCRCC with clear cell morphology, rich vasculature, and hemorrhage. Scale bar = 100 μm.

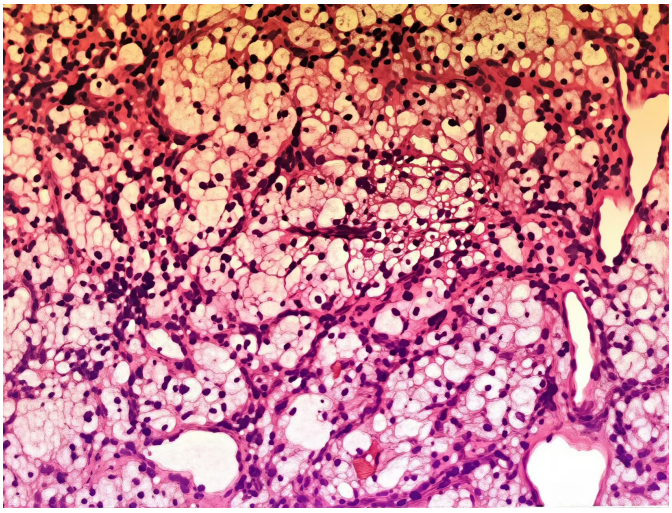

with numerous arteriovenous shunts, can disseminate to the head and neck via the paravertebral venous plexus (Batson's plexus) [7]. This mechanism underscores its significance as a rare cause of head and neck metastases unrelated to the upper digestive or respiratory tracts. Despite its relatively low overall incidence, priority should be given to considering it in the differential diagnosis of head and neck space-occupying lesions. In the absence of any other identified primary tumors, the clinical differential diagnosis for a patient presenting with a mass in the head and neck encompasses both benign lesions and malignant tumors, the latter including primary tumors and metastases. Benign tumors in this region typically exhibit slow growth and are often discovered incidentally. Their duration can range from several years to several decades [8]. In some patients, head and neck metastases may arise following radical nephrectomy for RCC, with time intervals varying from several months to several years. mCCRCC is associated with a poor prognosis, characterized by a 5-year survival rate of less than 10% and an average life expectancy of 5.8 months [1]. Research indicates that complete surgical resection of isolated metastases can significantly enhance the long-term survival rates of affected patients. O'Dea et al. investigated patients who underwent radical nephrectomy for RCC and had isolated metastatic sites completely excised. Their findings indicated that patients with metastases identified within a specific timeframe following nephrectomy exhibited a more favorable prognosis compared to those whose primary tumors and metastatic sites were diagnosed and treated concurrently. The 5-year survival rate for the former group was 50% [9]. Although RCC is characterized as a radioresistant tumor, it demonstrates a notable response to chemotherapy and radiotherapy. Moreover, the implementation of targeted therapy and immunotherapy can substantially enhance survival outcomes for patients [5]. The first case is notable for the deep lobe location and the synchronous lung metastases, underscoring the need for complete staging even when a head and neck mass appears isolated. The hypervascular imaging features (fast wash in/wash out on CT) mimicked a primary salivary gland tumour, but should raise suspicion for metastasis from a highly vascular primary such as RCC. The second case illustrates that ccRCC can recur after more than a decade, and isolated

head and neck metastases may be the first sign. Therefore, lifelong surveillance is mandatory after nephrectomy.

Most patients with mCCRCC initially present with clinical symptoms related to metastatic sites. Risk factors for this condition include older age, male gender, hypertension, smoking, and obesity. The absence of specific indicators in imaging studies and routine biological examinations complicates the differentiation of mCCRCC from the primary disease at the metastatic site, thereby hindering the development of an accurate treatment plan. Typical symptoms associated with tumors originating in the kidneys include hematuria, low back pain, and abdominal masses. However, in the case discussed in this article, the patient did not exhibit these characteristic symptoms during the initial visit; instead, the primary complaint was a painless mass in the head and neck. Postoperative pathological analysis confirmed the presence of a malignant tumor with renal metastasis. mCCRCC typically has a relatively insidious onset, and its clinical symptoms are often subtle. It is frequently diagnosed when patients undergo evaluation for various non-specific symptoms or other medical conditions. Determining whether a head and neck mass is primary or metastatic cancer can be challenging. Yu reported that the accuracy rate of ultrasound diagnosis for parotid gland tumors is only 78.6% [10]. The ultrasound characteristics of Case 1 in this article resemble those of benign tumors, suggesting a potential risk of misdiagnosis. To minimize the likelihood of misdiagnosis, a thorough medical history inquiry, careful consideration of the relationship between systemic and local factors, and a meticulous physical examination, including necessary general assessments, are essential for accurately determining the tu-

Table 1. The detailed clinical timelines for Case 1.

Date	Event	Clinical/Pathological Details
November 20, 2024	Symptom onset	Patient notices painless left preauricular mass
December 5, 2024	Initial presentation	ENT clinic visit; physical exam confirms 4 cm firm, mobile left parotid mass
December 6, 2024	Ultrasound	Left parotid: 3.2×2.8 cm cystic-solid lesion, well-circumscribed, rich vascularity (Grade 3 flow on color Doppler). **No FNA performed** due to high vascularity and differential including Warthin tumor
December 8, 2024	CT neck (contrast-enhanced)	Left deep parotid lobe: 3.6×2.3 cm heterogeneously enhancing mass with "fast-in fast-out" enhancement pattern, central cystic areas, peripheral vascular rim sign. **Differential:** Warthin tumor vs. salivary malignancy vs. metastatic hypervascular lesion
December 10, 2024	Preoperative labs	Normal renal function, no hematuria
December 18, 2024	Surgery	Left deep lobe parotidectomy with facial nerve preservation (monitored with NIM-Response 3.0). Intraoperative findings: 4.0×4.0×3.0 cm encapsulated, friable, highly vascular mass
December 18, 2024	Intraoperative frozen section	"Low-grade malignant salivary gland tumor" → prompted complete deep lobe resection with margin clearance
December 22, 2024	Final pathology	**Metastatic ccRCC:** Nested architecture, clear cytoplasm, delicate vasculature. Immunohistochemistry: PAX8(+), CAIX(+), CD10(+), Vimentin(+), CK7(-), p63(-), SOX10(-), Ki-67 10%
December 24, 2024	PET-CT staging	**Primary:** Left kidney lower pole cystic-solid mass 11.4×10.1 cm, SUVmax 5.86, perinephric fat invasion (T3a). **Metastases:** Left parotid (post-surgical bed, SUVmax 7.39), bilateral pulmonary nodules (The larger one is located in the posterior basal segment of the lower lobe of the left lung, approximately 1.2 cm, SUVmax 2.18), no bone or brain metastases
December 28, 2024	MDT consultation	Urology, oncology, radiation oncology. Decision: Systemic therapy first-line (pembrolizumab/axitinib), consider cytoreductive nephrectomy after 3 cycles if response
January 5, 2025	Treatment initiation	Pembrolizumab 200mg IV q3weeks + Axitinib 5mg PO BID (dose reduced to 3mg BID after 2 weeks due to grade 2 hypertension)
February 20, 2025	First restaging CT (8 weeks)	**RECIST 1.1:** Primary renal mass 8.3×7.4 cm (27% reduction, PR), pulmonary nodules stable (non-target). Parotid surgical bed clear. eGFR stable at 45 mL/min/1.73m²
April 2025	Ongoing	Continuous relief; alive

Note: Detailed clinical timeline for Case 1, illustrating the diagnostic trajectory from presentation with a left parotid mass through staging, surgical resection, and systemic therapy initiation. Key findings include characteristic hypervascular imaging features, definitive pathology confirming metastatic ccRCC with supportive immunohistochemistry (PAX8+, CAIX+), and favorable early response to pembrolizumab/axitinib combination therapy.

mor's nature.

The most prevalent histological type of RCC is ccRCC, which typically presents as nest-like transparent cells abundant in glycogen when examined under light microscopy. Its characteristic histological feature includes a rich network of interstitial blood vessels, with red blood cells often visible within the vascular lumen or between the nests of clear cells [11]. In histochemical analyses, RCC typically exhibits positive staining for glycogen and lipids. Immunohistochemical findings reveal a high expression rate of CD10 and Vimentin, which supports the diagnosis of RCC. Vimentin is predominantly expressed in mesenchymal tissue cells and tumor cells derived from mesenchymal tissue, while it is absent in normal epithelial cells. Historically, Vimentin served as a marker to differentiate mesenchymal tissue components from those of other origins. Recent literature has demonstrated that Vimentin is aberrantly expressed in the epithelial tumor cells of poorly differentiated carcinomas, indicating that this abnormal expression is closely associated with the invasive and metastatic potential of tumor cells [12-13]. CD10 exhibits strong positive expression primarily in normal renal balloon epithelial cells and proximal convoluted tubular epithelial cells, predominantly localized in the cell membrane with potential positivity in the cytoplasm below. Its positive presence in mCCRCC correlates with advanced

Table 2. The detailed clinical timelines for Case 2.

Date	Event	Clinical/Pathological Details
May 2011	Initial diagnosis	Left nephrectomy for pT2aN0M0 ccRCC, Fuhrman grade 2, clear cell type
2011-2024	Surveillance	Annual abdominal CT and chest X-ray, no recurrence detected
April 1, 2025	Symptom onset	Foreign body sensation right oropharynx
May 6, 2025	ENT evaluation	Laryngoscopy: 1.0×1.0 cm smooth reddish mass, right lateral pharyngeal wall
May 8, 2025	Surgery	Laryngoscopic transoral resection of right oropharyngeal mass with 5mm margins. Intraoperative findings: Highly vascular, friable red mass
May 8, 2025	Intraoperative frozen	Consistent with metastatic ccRCC (clear cells, rich vasculature)
May 12, 2025	Final pathology	ccRCC metastasis, negative margins (R0), lymphovascular invasion present
May 15, 2025	MDT consultation	Medical oncology recommendation: Adjuvant systemic therapy with nivolumab/cabozantinib (preferred for intermediate-risk recurrence) vs. observation (high-risk for further metastasis given 14-year latency suggesting aggressive clone)
May 20, 2025	Treatment decision	Patient elected active treatment. Initiated Nivolumab 240mg IV q2weeks + Cabozantinib 40mg PO daily (dose reduced to 20mg due to baseline CKD)
July 2025	First restaging (8 weeks)	**RECIST 1.1:** No measurable disease (post-surgical), no new lesions. Treatment continued as adjuvant approach
September 2025	Ongoing	Stable, no progression

Note: Detailed clinical timeline for Case 2, illustrating an ultra-late recurrence (14 years post-nephrectomy) of ccRCC manifesting as isolated oropharyngeal metastasis. The timeline encompasses the 14-year disease-free interval, diagnostic workup, complete surgical resection, and initiation of adjuvant immunotherapy-based systemic treatment, highlighting the importance of prolonged surveillance in ccRCC survivors.

Table 3. A summary of the most relevant published cases.

Reference	Age/Sex	Site	Time from nephrectomy	Other metastases	Outcome (follow up)
Owens et al. 1989 [9]	55/M	Parotid	0 (synchronous)	Lung, brain, bone	Alive at 2 years
Owens et al. 1989 [9]	75/F	Parotid	8 years	None	recurrence (6 months after parotid resection)
Spreafico et al. 2008 [7]	67/M	Parotid	1 years	neck lymph nodes	Alive, radiotherapy
Ahmed et al. 2023 [5]	66/M	Larynx	0 (synchronous)	None	Alive, NED at 4 months
Present Case 1	61/M	Parotid (deep lobe)	0 (synchronous)	Lung	Alive, on IT at 10 months
Present Case 2	69/M	Oropharynx	14 years	None	Alive, NED at 8 months

Note: Comparative summary of published ccRCC head and neck metastasis cases, highlighting the rarity of deep parotid involvement (Case 1) and the unprecedented 14-year latency for oropharyngeal recurrence (Case 2) among reported series.

tumor stage, suggesting involvement in invasion and progression. Notably, poorly differentiated mCCRCC tumors display a significantly lower CD10 expression rate compared to moderately and well-differentiated tumors, indicating a link between CD10 expression and mCCRCC cell differentiation [14]. From a pathological perspective, a definitive diagnosis of mCCRCC requires a panel of IHC markers. PAX8 is the most sensitive and specific marker for renal origin. CD10, and vimentin are supportive but not entirely specific. Exclusion of salivary gland tumours (p63, p40, S100, SOX10) and other clear cell neoplasms (e.g., from thyroid, adrenal, or female genital tract) is essential [14]. Ki 67 provides prognostic information. In our cases, the IHC profile was classic for ccRCC and ruled out mimics.

Our report has limitations. First, we lack long term follow up for both patients, especially regarding treatment response beyond 10 and 8 months. Second, the decision not to perform FNAC in two cases might be debated; however, in many centres, surgical excision is preferred for deep parotid lesions when malignancy is suspected, because FNAC can be non diagnostic or misleading. Despite these limitations, these cases contribute valuable observations: (1) ccRCC can present as a parotid deep lobe mass, which has not been specifically highlighted before; (2) a latency of 14 years before oropharyngeal metastasis is one of the longest reported; (3) hypervascular imaging features should prompt consideration of ccRCC; (4) a comprehensive IHC panel is crucial for accurate diagnosis.

Conclusion

In summary, instances of mCCRCC spreading to the head and neck are exceedingly uncommon, representing only approximately 6% of cases [15]. mCCRCC should be included in the differential diagnosis of hypervascular head and neck masses, even in patients without known renal cancer or with a remote history of nephrectomy. The diagnosis relies significantly on identifying the distinct pathological characteristics of metastatic cancer through meticulous IHC analysis. The presence of CD10 and Vimentin positivity aids in confirming the diagnosis of mCCRCC. When encountering clear cell carcinoma in pathological samples, consideration must be given to the potential metastasis of RCC. Timely PET-CT and a thorough immunohistochemical work up are essential for correct diagnosis and staging. Patients typically do not exhibit evident symptoms like hematuria or lumbar pain. Merely excising the metastatic cancer lesions does not result in complete remission. Prompt initiation of MDT consultations is essential, with a comprehensive treatment approach primarily centered on radical surgical excision. Regular and lifelong monitoring should also be implemented. The primary lesions associated with head and neck metastatic cancer predominantly arise from the upper digestive and respiratory tracts, with a minority originating from distant organs. Specifically, 45% of metastatic cancers are classified as malignant melanoma, while 37% are identified as squamous cell carcinoma. Distant metastatic cancers may also originate from sites such as the breast, kidneys, and prostate [16]. For the majority of these patients, a definitive diagnosis is achievable only through postoperative pathological examination. Consequently, in clinical practice, it is advisable to extend the follow-up period for patients with mCCRCC as much as possible. In cases where patients present with head and neck masses without identifiable tumors in that region, primary tumors located below the clavicle should be considered, prompting the initiation of appropriate staging examinations. For isolated metastatic lesions, surgical intervention may be indicated. Additionally, postoperative immunotherapy or molecular targeted therapies can be employed to extend patient survival and enhance quality of life.

Abbreviations

chromophobe renal cell carcinoma : chRCC; metastatic clear cell renal cell carcinoma : mCCRCC; papillary renal cell carcinoma : pRCC; Renal cell carcinoma: RCC; Clear cell renal cell carcinoma: ccRCC; FNAC: fine needle aspiration cytology; IHC: immunohistochemistry; PET-CT: Positron Emission Tomography-Computed Tomography; CAIX: carbonic anhydrase IX; MDT: multidisciplinary team; RECIST: Response Evaluation Criteria in Solid Tumours; TNM: tumour node metastasis.

Author Contributions

Xinyao Han drafted the manuscript and collected clinical cases. Hui Huangfu performed the operation on the patient and participated in revising this manuscript. All authors read and approved the final manuscript.

Acknowledgements

I am grateful for the assistance provided by my mentor. We acknowledge the patient's contributions to the study.

Funding Information

Not Applicable

Ethics Approval and Consent to Participate

This study was reviewed and approved by the Research Ethics Committee of First Hospital of Shanxi Medical University with the ethical code KYLL-2025-429 on 24 November 2025.

Competing Interests

The authors declare that they have no existing or potential commercial or financial relationships that could create a conflict of interest at the time of conducting this study.

Data availability

Not Applicable

References

[1] KWEON H T, YOO J S, HONG Y T. Tongue Metastasis From Renal Cell Carcinoma: A Rare Case Presentation[J/OL]. Ear, Nose, & Throat Journal, 2024: 1455613231226038. https://doi.org/10.1177/01455613231226038

[2] Linehan, W. M., & Ricketts, C. J. (2019). The Cancer Genome Atlas of renal cell carcinoma: findings and clinical implications. Nature reviews. Urology, 16(9), 539–552. https://doi.org/10.1038/s41585-019-0211-5

[3] Gao, S., Yan, L., Zhang, H., Fan, X., Jiao, X., & Shao, F. (2021). Identification of a Metastasis-Associated Gene Signature of Clear Cell Renal Cell Carcinoma. Frontiers in genetics, 11, 603455. https://doi.org/10.3389/fgene.2020.603455

[4] Lalani, A. A., McGregor, B. A., Albiges, L., Choueiri, T. K., Motzer, R., Powles, T., Wood, C., et al. (2019). Systemic Treatment of Metastatic Clear Cell Renal Cell Carcinoma in 2018: Current Paradigms, Use of Immunotherapy, and Future Directions. European urology, 75(1), 100–110. https://doi.org/10.1016/j.eururo.2018.10.010

[5] Ahmed, S. S., Barik, S. K., Adhya, A. K., Das, D. K., Parida, A. V., Mukherjee, P., Das Majumdar, et al. (2023). Metastatic Renal Cell Carcinoma Masquerading as a Laryngeal Tumor: A Case Report. Cureus, 15(5), e39229. https://doi.org/10.7759/cureus.39229

[6] Lieder, A., Guenzel, T., Lebentrau, S., Schneider, C., & Franzen, A. (2017). Diagnostic relevance of metastatic renal cell carcinoma in the head and neck: An evaluation of 22 cases in 671 patients. International braz j urol : official journal of the Brazilian Society of Urology, 43(2), 202–208. https://doi.org/10.1590/S1677-5538.IBJU.2015.0665

[7] Spreafico, R., Nicoletti, G., Ferrario, F., Scanziani, R., & Grasso, M. (2008). Parotid metastasis from renal cell carcinoma: a case report and review of the literature. Acta otorhinolaryngologica Italica : organo ufficiale della Societa italiana di otorinolaringologia e chirurgia cervico-facciale, 28(5), 266–268.

[8] Wang Jibao, Kong Weijia, Huang Xuanzhao. Practice Of Otorhinolaryngology Head and Neck Surgery [M]. 2nd ed. Beijing: People's Medical Publishing House, 2008: 653

[9] Owens, R. M., Friedman, C. D., & Becker, S. P. (1989). Renal cell carcinoma with metastasis to the parotid gland: case reports and review of the literature. Head & neck, 11(2), 174–178. https://doi.org/10.1002/hed.2880110212

[10] Yu GY (ed): Salivary Gland Diseases. Beijing Medical University Press, Beijing, 1994.

[11] Majewska, H., Skálová, A., Radecka, K., Stodulski, D., Hyrcza, M., Stankiewicz, C., et al. (2016). Renal clear cell carcinoma metastasis to salivary glands - a series of 9 cases: clinico-pathological study. Polish journal of pathology : official journal of the Polish Society of Pathologists, 67(1), 39–45. https://doi.org/10.5114/pjp.2016.59475

[12] Singh, S., Sadacharan, S., Su, S., Belldegrun, A., Persad, S., & Singh, G. (2003). Overexpression of vimentin: role in the invasive phenotype in an androgen-independent model of prostate cancer. Cancer research, 63(9), 2306–2311.

[13] Lang, S. H., Hyde, C., Reid, I. N., Hitchcock, I. S., Hart, C. A., Bryden, A. A., et al. (2002). Enhanced expression of vimentin in motile prostate cell lines and in poorly differentiated and metastatic prostate carcinoma. The Prostate, 52(4), 253–263. https://doi.org/10.1002/pros.10088

[14] Shaoxiong Ming. (2014). Expression and Clinical Significance of CD10 in Renal Cell Carcinoma [Master's thesis, Nankai University]. http://dx.chinadoi.cn/10.7666/d.Y2699723.

[15] F Higuera, L A Boccalatte, M J Labanca, A Jaén del Valle, J J Larrañaga, M F Figari, Renal clear cell carcinoma metastasis to submandibular gland: case report and review of the literature, Journal of Surgical Case Reports, Volume 2018, Issue 10, October 2018, rjy261, https://doi.org/10.1093/jscr/rjy261

[16] Hongchi Xue, Jinhua Yu, Yan Gao, & Minxian Huang. (2000). Renal clear cell carcinoma metastasis to the parotid gland: A case report. Journal of Modern Stomatology. 14(1), 38. http://dx.chinadoi.cn/10.3969/j.issn.1003-7632.2000.01.043.